Dynamic Visual Communication Image Framing of Graphic Design in a Virtual Reality Environment

ZHIYONG TIAN [iD]

College of Arts, Henan University of Animal Husbandry and Economy, Zhengzhou 450000, China

e-mail: tzy19811008@163.com

ABSTRACT This paper explores dynamic visual communication image framing for graphic design based on virtual reality algorithms; it defines corresponding feature representations by delineating layers of pixels, elements, relationships, planes, and applications; and it investigates methods for quantifying geometric features, perceptual features, and style features. The contents include extraction methods for element colors, calculation methods for layout perceptual features and color-matching perceptual features, and pairwise comparison methods for style features. By overfitting the distribution of geometric features in the data, the model can predict the probability density distribution of features such as element position and color under specific conditions to support the generation of flat images. To construct a prediction model, the sampling method of features, the model optimization method, and the data learning strategy are investigated. This thesis involves the design and implementation of a lossless/near-lossless compression system for high-frame-rate gaze camera image data, which is faced with the technical problems of high fidelity and strong real-time and reliable compression. The image single-frame lossless/near-loss-free compression ratio is generally low, and the compression ratio can be improved by using the correlation between image frames. In this paper, we study the application of lossless compression between image frames, the efficient computing structure of FPGA, and an onboard compression system.

INDEX TERMS Virtual reality, graphic design, dynamic visual communication, image framing.

I. INTRODUCTION

With the rapid development of digitalization, the interoperability of mobile phones, computers, the Internet, and other media provides designers with more freedom and more space in which to play. There is a continuous enrichment of new media that injects fresh perspectives into new communication concepts and the diversification of communication forms, thereby opening up a new path for the form of graphic design [1]. In this era of new media digitalization, dynamic graphics can be applied in many design fields regardless of whether they are planar or nonplanar; they can be used reasonably and will be sought after by designers [2].

With the increasing number of dynamic design works, people are unsatisfied with watching a simple dynamic effect. It is

The associate editor coordinating the review of this manuscript and approving it for publication was Zhihan Lv [iD].

better to create the content of the context through dynamic effects, the most direct of which impart information related to feelings. Take the current elevator advertising format for example; previously, posted advertising pages were given priority, but in recent years, it has become rare to see these traditional posters, as most advertising is now in the laddering format [3]. The main form of advertising communication, the original static scene performance, has been dynamically reconstructed. From static to dynamic, the shaping of the situation is now more realistic, and the information is conveyed more quickly and is more adaptable to the development trend of new media to tease the viewer's vision and attract more attention [4].

The situation created by dynamic graphics is more in line with the audience's pursuit of the prototype and the maximization of the user experience [5]. Dynamic graphics provide a good space for the performance of the context, and

the dynamic contextual language is more accurate so that the information can be more accurately transmitted to the audience. The unique dynamic spatial and temporal dimension effectively enhances the immersion and tension of the contextual performance, which can maximize the distance between the work and the audience [6].

Li SC *et al.* perceived students' gaze changes by placing eye movement devices in the classroom to understand students' attention span and distractions [7]. However, eye movements are not the best way to transmit emotions; rather, they are a partial way to identify emotions [8]. For the physical manifestation of emotions, human brain waves and heart rates are a good basis for emotional discrimination [9]. Brengman classified human emotions by studying the universal meaning of facial expressions and exploring the association between expressions and a definite emotion beforehand and proposed six basic emotions namely, happiness, sadness, surprise, fear, disgust, and anger, each of which corresponds to unique facial features [10].

By delineating the facial muscle movement patterns of different expressions, research experts have in turn proposed a facial movement coding system, which has greatly facilitated the research process of computer analysis of facial images of human faces [11]. For the extraction of facial expressions, which are mainly divided into two types (dynamic sequences and static images), the facial features of static images are mainly described by the image texture; for example, Tom Dieck D used the Viola-Jones framework and principal component analysis to extract the static features that identify facial expressions [12].

Dynamic sequences of features focus more on the shifting of facial feature coordinates such as the movement of the corners of the mouth when the face is smiling [13]. Izzo F used 12 action units as dynamic features to reduce the number of features and make the emotion recognizer more efficient by using feature selection algorithms such as generative algorithms and simulated annealing after generating feature values on the face image [14]. As an effective expression of emotion, the expression is an intuitive and easily perceptible epiphenomenal feature, and the slightest changes in key facial regions can reflect an individual's immediate state of mind; therefore, effectively capturing features and changes in facial information is an important prerequisite for our analysis of individual emotion dynamics [15].

To improve the accuracy of facial expression classification, Qin L added a batch specification (BN) layer to the original network using the batch specification idea to make the recognition accuracy higher than that of the original network [16]. Neural networks require a large amount of training data to obtain the prerequisites for good training; however, the current publicly available expression datasets have problems such as low number and incomplete sample classification, which greatly affect the network performance and thus solve the neural network problem. With regard to insufficient numbers of training samples [17], Park JH *et al.* performed the complex processing of training samples to

form multiview samples and trained the model on neural networks in the use of migration learning and multiviews. They ultimately obtained better recognition [18].

Buonincontri P *et al.* greatly reduced the training parameters and improved the efficiency of expression recognition by adjusting the number of feature maps in the convolutional layer and the number of nodes in the fully connected layer in the classical network model [19]. Although there has been a great deal of research on expression recognition, there is still much room for improvement in the study of human emotion analysis due to the current situation, such as interference from external conditions and different relationships between different individual emotions and expression mappings [20].

In this paper, a fusion of interframe lossless and near-lossless image compression methods is proposed to address the two main problems of ''high-fidelity image compression under finite bandwidth constraint'' and ''high real-time image compression under finite resource constraint'' in the field of Earth observation. In this paper, the compression method utilizes the interframe pixel information of remote sensing images, which can eliminate the temporal and spatial redundancy, improve the compression ratio, and reduce the bandwidth pressure based on high-fidelity image compression. For geostationary transmission, we study the hardware computing architecture for efficient real-time compression and to design a highly reliable image compression system.

Whether the introduction of virtual reality education in the current situation is more beneficial to current high school art appreciation courses is a question worth investigating. The blind pursuit of high-end educational technology will lead to a decline in teaching quality. With the continuous development of virtual education, virtual reality should be combined with traditional education to enhance advantages, avoid disadvantages, and target teaching activities in secondary art education. Through virtual reality art education, students and teachers can better carry out the new era of information education and innovation education, develop multidomain teaching resources, effectively cultivate interdisciplinary core literacy, and enrich education and teaching methods to promote the development of art education.

II. GRAPHIC DESIGN SYSTEM DESIGN IN VIRTUAL REALITY ENVIRONMENT
A. VIRTUAL REALITY SYSTEM DESIGN
The new media trend provides a good environment and convenient channels for the development of dynamic design [21]. From the function, the information brought by dynamic graphic language is dynamic, which can make the audience accept the information more clearly in a short period. At the same time, it is more interesting than general graphic design, so it is more widely used by designers and accepted by the audience. From the application scope, the dynamic graphic language is widely used. It can be well integrated into the design field in all directions, and it can also be used in the field of design [22]. Through silent language, the system can break geographical boundaries, language fetters, and cultural
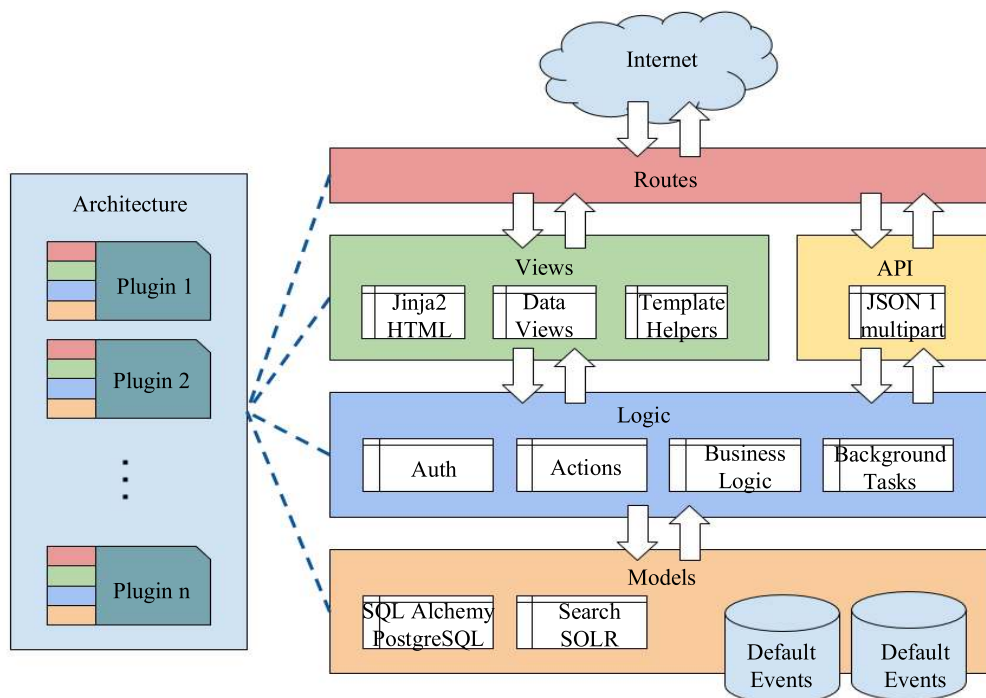
FIGURE 1. Virtual system framework diagram.

differences; it can instantly shorten the distance between the viewer and the work; and it can achieve the most rapid and convenient communication. From function, the diverse functions of the DGL can not only quickly attract the viewer's attention but also shuttle between the work and the viewer as a carrier of mutual emotional response, as shown in Figure 1.

In this paper, we introduce the virtual roaming system, which is divided into three parts: Kinect, PC, and VR. Kinect is responsible for acquiring the user's skeleton position, PC is responsible for selecting key points and defining the virtual boundary of tracking space, and VR is responsible for the motion correlation between virtual walking and real walking, as shown in Figure 1. First, we use Kinect to capture the user's skeleton position and transmit it to the PC terminal for data processing [23]. Then, we select the spine node as the user's key point from several skeleton nodes in the PC terminal, determine the virtual boundary of the tracking space based on the initial key point position of the user in the Kinect system, and design an algorithm to calculate the displacement of the user's key point and transmit the displacement and real-time position of the key point to the VR terminal via the socket method.

Finally, we consider the user wearing the VR device and the tracking space as the components of the VR terminal. In the VR terminal, the user walks in the tracking area, but the visual display shows that the user walks in the virtual space, in which there are motion correlations between the virtual space and the real space [24]. In the virtual space, we use the offset obtained from the PC terminal to drive the virtual spacewalking and generate the Voronoi path corresponding to the virtual space and extract the path information

to guide walking in the tracking space. In the tracking space, we use the direction information obtained from the gyroscope and the real-time position information obtained from the PC terminal to calibrate the user's real walking to avoid user information in the tracking area. The calculation of the algorithm generates cumulative errors, and the real walk includes two states: the three-level arc walk and the dynamic steering during the reset [25].

The kernel density estimation (KDE) method is a nonparametric method for estimating probability density as proposed by Rosenblatt and Emanuel Parcen. The method uses a smooth kernel function to fit the observed data points and thus a probabilistic fit to the true distribution curve [26]. Since this method does not take advantage of the a priori knowledge of the distribution of the data in question and makes no assumptions about the data distribution, it is often used to characterize the distribution of the data samples themselves. Assuming that there are two mutually independent sample points, the distribution of these sample points is F(x), and the probability density function is f(x). Then, [27] exists as follows:

$$F(x) = \int_{-\infty}^{x} f(m)dm \qquad (1)$$

where f(x) denotes the probability of the sample appearing at that point. Since the probability density function is the first-order derivative of the distribution function, the fundamental theorem of derivatives can define h.

$$f(x) = \lim_{h \to \infty} \left(\frac{F(x+h) - F(x-h)}{2h} \right) \qquad (2)$$
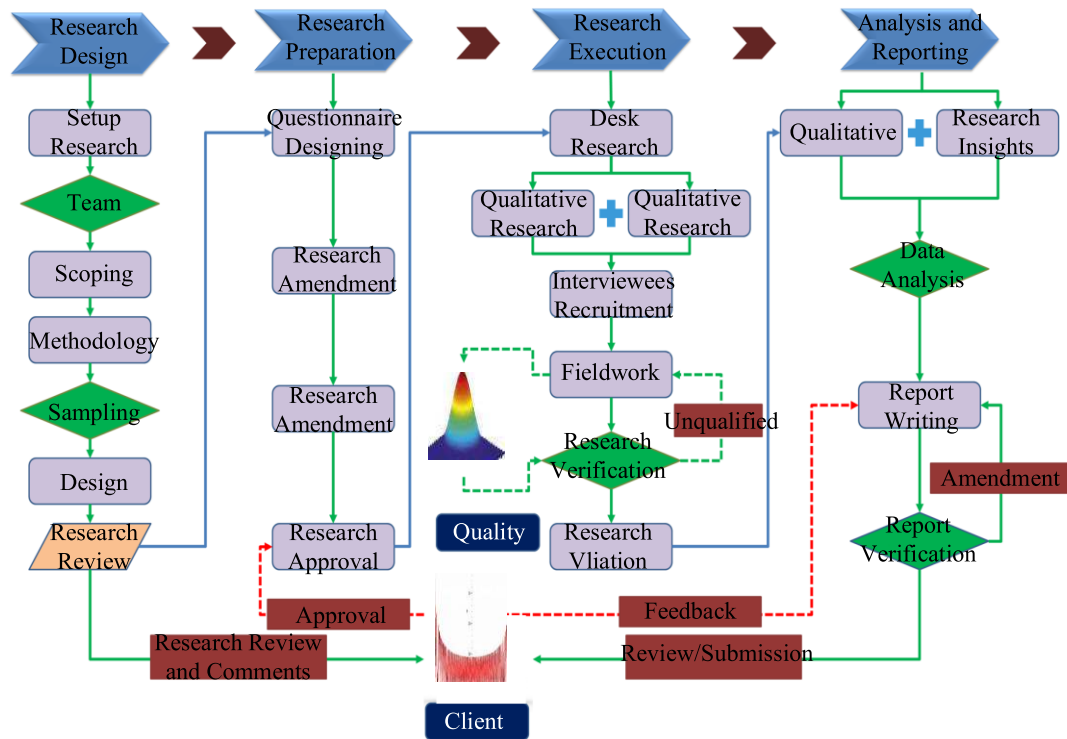
FIGURE 2. Probability density distribution of background colors for different keywords.

Since the true distribution F(m) is unknown, an empirical distribution function can be used to approximate F(x):

$$\bar{F}_n(m) = \frac{1}{n}\sum_{i=1}^{n} 1_{x_i \leq t} \qquad (3)$$

$$\bar{F}_h(x) = \frac{1}{nh}\sum_{i=1}^{n} K\left(\frac{x - x_e^i}{h}\right) \qquad (4)$$

Among them, K is a nonnegative nuclear function, and k is a smoothing parameter, also known as the bandwidth. To ensure the integration of the density function for 1, the original nuclear function F can be replaced by other distributions of the density function including the common uniform nuclear function, trigonometric function, gamma function, and Gaussian nuclei function. These nuclear functions are used to meet the integration of 1, the mean value of 0, and other characteristics [28].

Bandwidth will also affect the final fit of the function. The larger the bandwidth is, the smaller the proportion of the observed data points in the final curve shape is and the flatter the overall KDE curve is. The smaller the bandwidth is, the larger the proportion of the observed data points in the final curve shape is and the steeper the overall KDE curve is [29]. There are many ways to select the bandwidth, and cross-validation is one of the commonly used selection methods. During the construction of the probability density function, the data can be divided into two parts: one for fitting and the other for validation. By comparing the validation results of multiple bandwidth values, the bandwidth with the

least error is used as the smoothing parameter of the function:

$$\bar{F}_H(x) = \frac{1}{n |H|^{1/2}} \sum_{i=1}^{n} K\left(\frac{x - x_e^i}{H^{1/2}}\right) \qquad (5)$$

The nuclear probability density function can be used to model the design features sampled in the dataset to estimate the distribution law of specific design features. Specifically, to analyze the color design features of different brands of print advertising images, it is possible to collect images of different brands of print advertising and then model the color features in the images with nuclear density estimation [30]. Figure 2 shows the color feature modeling results of images related to the keywords "618" and "MUJI." Since the background of a graphic design image often occupies the largest color representation area, the algorithm transforms the dominant color in the background element into CIELab color space and builds a multidimensional variable density estimation distribution map based on the color feature data sampled by the a∗b∗ channel value.

On the left side of Figure 2 is a sample print ad image corresponding to the keyword. In the middle is a visual distribution map with the color feature of the a∗b∗ channel as the axis, and on the right side is the color corresponding to the a∗b∗ channel value. As we can see from the results, the print image background of the campaign theme is more likely to use red and purple colors to create a festive atmosphere, and the print image background of the "MUJI" brand is mainly gray and white to strengthen the brand's visual impression in the target users' mind and consolidate the brand culture.

The conditional probability density function can be used to fit the relationship between two features to estimate the probability distribution of the target design features under the condition of a design feature [31]. Taking the text color in a print advertising image as an example, Figure 2 shows the results of the kernel density estimation of the luminance features of the text color computed based on the chapter approach. From the results, there are high probability density distributions for different font luminance features. Such a distribution function has difficulty helping the computer determine the applicable font luminance features to guide the generation of flat images. The reason there are such distribution results is that there is a strong correlation between the background and font color in the graphic design image [32]. This correlation is mainly manifested in the high contrast between the colors to enhance the effect of the font's information conveyance in the image. To improve the convergence of the distribution, the color features of the background in the copy elements can be used as conditions to construct the corresponding conditional probability density function to estimate the probability distribution of the text color features.

Figure 2 shows the distribution of text color luminance for different background luminance features (the lower color in the figure is the background color). From the results, it can be seen that on a darker background (e.g., when the background luminance is 0.2), the text color is more likely to be brighter. On a brighter background (e.g., when the background color luminance is 0.9), the text color is mostly below 0.5. When the background luminance is in the middle region, not only can we probabilistically use a high-brightness text color, but we can also use some appropriate low-luminance colors. Compared to the kernel density estimation method, some of the features of a graphic design image will be more convergent under conditional probability estimation. The more convergent results are also more design-directed for the computer.

B. GRAPHIC DESIGN DYNAMIC COMMUNICATION DESIGN

In terms of the dynamic graphic language itself, disseminating information for textual information can be summarized and refined into a way that can be used to explain the information content through contextual performance. Compared to boring language, dynamic language is more expressive and more conducive to recognition and memory, and it is more likely to attract the audience in the form of actively received information. With mobile Internet development, the speed, capacity, and scope of information dissemination are fast, and under the influence of such large amounts of information, the audience has more ways to learn, and the aesthetic level also improves; thus, it is easy to produce aesthetic fatigue. Thus, traditional static, two-dimensional graphic expressions can no longer meet the visual aesthetic needs of viewers, and new creative elements need to be added to create rich works [33]. The expression of traditional graphic design is not flexible or full enough, nor does it have enough tension or standardization in regard to the expression of the work;

however, traditional static graphic design can become more versatile and flexible. Its combination with dynamic design becomes the best choice for the development of graphic design, and the development of dynamic design is the trend.

Dynamic graphics, as a product of graphic design and animation design, have a close relationship with animation design; i.e., they are both composed of a continuous picture and are a simple form of animation. Both are composed of dynamic design, graphic design, and time design, but the proportion of components is not the same. In dynamic graphic design, graphic design occupies the main position, and dynamic form and time design are second. In animation design, dynamic design occupies the main position, and time design is second to graphic design. Dynamic graphic design mainly emphasizes the output of information, which is also the main visual communication design. Function leans more toward expressing the idea of design, whereas animation focuses on whether the story is logical and complete. Therefore, as more media enter the picture, the development of motion graphics expands more widely, as shown in Figure 3.

This kind of kinetic effect can reduce the production cost and operation difficulty compared with animation and 3D effects and shorten the time accordingly.

In graphic design, words have the characteristics of ideograms, which is the most direct and accurate element to tell the content of works, but some emotional expressions cannot be fully explained by words alone. The deeper connotation cannot be told directly, so if you want viewers to understand it without expressing it through words, then the most appropriate way to design works is to create a contextual expression [34]. At the same time, there are various ways of contextual expression, with strong technical support, and different semantics can be expressed in different contextual expressions. This causes greater tension in design and provides a situation in which designers' unimaginative ideas can be wielded freely. Symbolism is one of the artistic features of motion graphics design as well as one of the aesthetic characteristics of motion graphics contextual expression.

Symbolic performance is usually easy to understand. Graphics, colors, and characters can be the symbolic representatives of the situation. For example, red represents hot and unrestrained, purple represents melancholy and mystery, yellow represents positive sunshine, the circle is representative of roundness, the polygon is the representative of personality and angles, straight lines give people a calm and soothing mood, and curves cause turbulence. These symbols are indispensable in visual works and situations where important elements shape the support. In motion graphics design, the existence is no longer merely flat, and its symbolic expression is more multidimensional.

These symbols can be used to convey information more quickly in contextual representations, and the language of these symbols is highly refined and representative of the designer [35]. The mascot, as the spokesperson of the brand, can quickly convey the characteristics of the company, brand, or product through the refined shape of the mascot, which
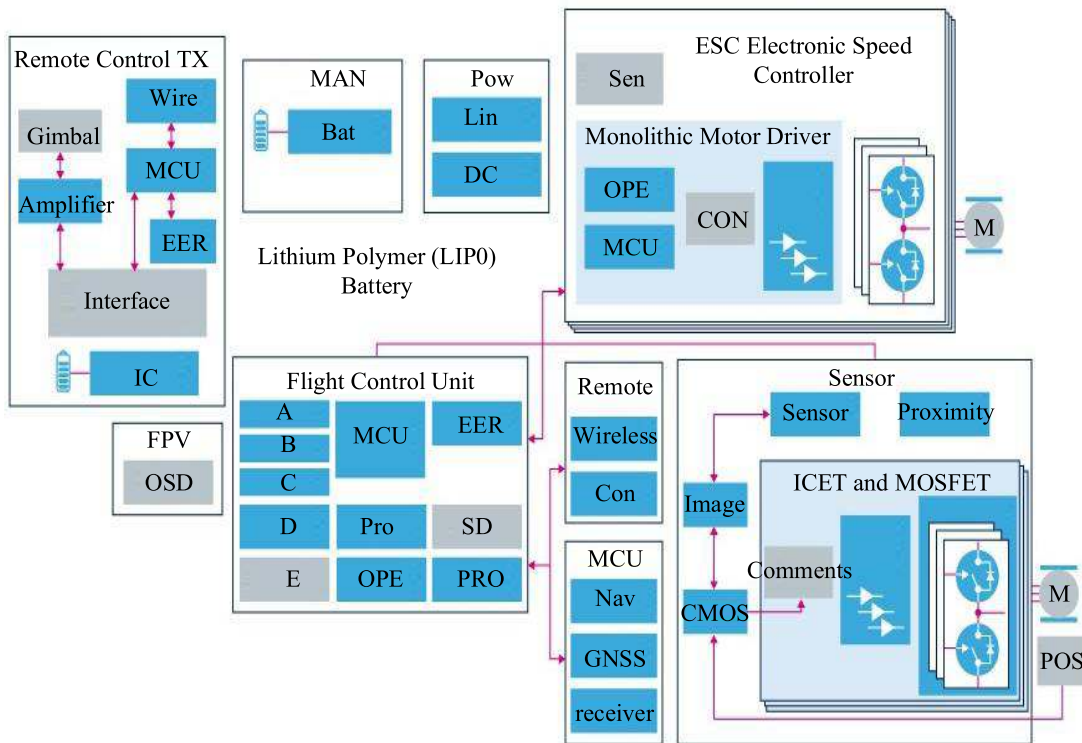
FIGURE 3. Graphic design dynamic communication design framework.

will have different appearances or movements in different situations or themes. The effect is crisp and simple, quickly catching the audience's eye and triggering fun consumption. Now, consumption is not only as simple as buying goods but also, and more importantly, involves the consumption of brand concept and brand aesthetic identity; thus, symbolic aesthetic characteristics are still very important here.

In the contextual representation of dynamic graphics, whether it is real, expressive, or symbolic, all are served for better output content, and only the joint action of dynamic graphics and contextual representation can show the work more effectively.

III. DYNAMIC VISUAL COMMUNICATION IMAGE FRAMING
A. DYNAMIC VISUAL COMMUNICATION IMAGE GENERATION DESIGN
The design feature-driven planar image generation method can construct a corresponding probabilistic model based on the design features from different training data. The optimal features predicted by the model can not only guide the image layout generation but also serve as target features for the color reconstruction of the image. In this chapter, we introduce the clustering and visualization methods of features from the perceptual features of flat images to construct training data for different design requirements. On this basis, the image layout generation method for graphic blending and the image color reconstruction method for dominant color guidance are further introduced to output the final graphic advertising image. Finally, user perception evaluation and
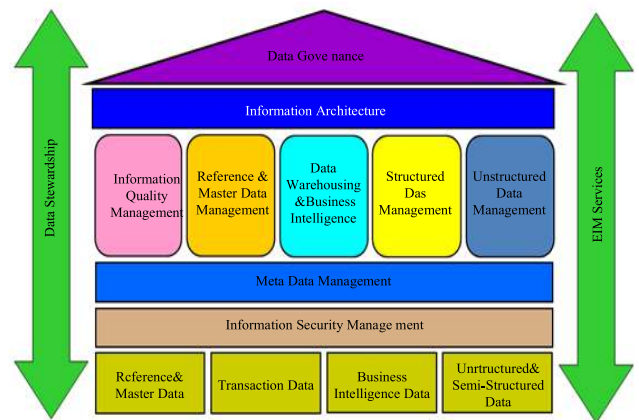

FIGURE 4. Main structure and content framework.

comparison experiments are used to analyze the design results of the graphic advertising images, verify the effectiveness of the method, and discuss the corresponding shortcomings. The main structure and content are shown in Figure 4.

The rise of new media has brought great convenience to the audience with two windfalls; the first is the emergence of the WeChat public platform in regard to the creation of a large wave of self-employment and the successful acquisition of wealth in the new media, and the second is the speed and convenience of the audience's mobile access to information on which they increasingly rely as a way to draw knowledge.

In print advertising images, the positional relationships between elements can be clustered to quantify different layout perception features. These clusters include a left-right

layout, centered layout, and top-down layout. The layout-aware features obtained from the different clusters describe a layout style and can be used to generate diverse layout design results. Additionally, considering that there is also a large amount of textual content in the form of characters in the image, this subsection describes the layout generation method for multiple lines of text based on the container design features obtained from the model estimation for the final print advertising image layout generation.

To generate diverse layout design results, the positional relationships between elements in the image can be clustered to construct different training sets. In this paper, the layout clustering algorithm shown in Algorithm 2 is used to categorize the layout styles of the graphic advertising images in the dataset. Figure 4 shows the interactive interface generated by diverse layouts. Each layout clustering result is presented visually as an estimation of the container layout features. The black rectangle is the image container, and the gray rectangle is the copy container. The percentage below represents the recommendation index, calculated based on the proportion of the cluster in the dataset. After the designer selects a layout cluster, the algorithm will use the planar image of the cluster as training data to construct the corresponding element geometric feature model to estimate the layout geometric features of the container.

Since planar images in the same cluster tend to have more similar layout geometric features, this cluster-specific feature learning approach can not only meet diverse design requirements but also improve the convergence of the model fit to some extent. Additionally, for print advertising images that contain two or more copy containers in the image, the algorithm will perform further layout clustering based on the location relationships of multiple copy containers to provide more design options.

Using the introduced method of estimating the geometric features of the container layout, the layout design task of the image class elements can be achieved. However, in practical graphic design tasks, textual content in the form of characters is more easily adapted to image content. These input characters are often in behavioral units. Each unit of text has specific element character features such as character text for the main title, subtitle, and product description. Since the readability of the text content is an important indicator for evaluating design quality, the relationship between text size and content importance, as well as the relationship between text semantics and layout location, needs to be considered when implementing multiline text layout generation.

The text characters have different design characteristics according to different languages. Since most of the graphic advertising design images collected in this paper come from large domestic e-commerce websites such as Taobao and Tmall, the text in the images is mostly in Chinese. Therefore, when implementing the multiline text layout of the element container, the algorithm assumes that all input characters are Chinese, and each character has the same length and width.

On this basis, the algorithm further optimizes the layout geometric features of the input characters concerning the layout perceptual features such as alignment, boundary, unity, and white space, combined with the element importance. Specifically, the algorithm first optimizes the layout of unbalanced characters per line in each copy element. For elements where the difference in the number of characters between lines is greater than the minimum number of characters in one of the lines, the algorithm will adjust the number of characters per line until the threshold requirement is met. Additionally, based on the manually specified and labeled significant areas of the image (e.g., the model's face and product areas are significant), the algorithm will modify the geometric features of the copy layout placed above the significant areas to place them below the significant areas to avoid degrading the content information conveyed by the print ad image.

Color is an important factor in the aesthetic perception of users. Different target users often have different preferences for color. For example, warm colors can produce a warm and comfortable feeling, while cool colors can give people a cool and fresh feeling. This section introduces a visualization method based on t-SNE for the perception of color matching features. In the visualization interface, the designer can easily cluster images to select flat images with specific color styles and train the corresponding geometric feature models. At the same time, based on the elemental primary color features output from the model, this section introduces related image color reconstruction methods, including chroma feature adjustment and luminance feature adjustment, to complete the final color design of the print advertising image.

Selecting training images with specific color styles can help the model better fit the color geometric features. Since direct image filtering is inherently inefficient and the color relationships between images cannot be expressed, visualizing the perceptual features of an image's color scheme becomes an effective form of interaction. To help designers visualize the color relationships between images, this section uses t-SNE to visualize the color-perceived features of images.

B. IMAGE FRAME FIXATION EVALUATION INDEX DESIGN

The establishment of contextualization will inevitably lead to a corresponding interaction between people and works, which is also a unique feature of dynamic graphic design itself. In the digital era, with the addition of new media and new technologies, collaborations with dynamic graphic design presents new ways of expression and interaction. This enhances the experience of reality and brings a unique form of contextual expression that includes two forms of interaction, one of which is the interaction between people and works. There is also interaction between people and technology. The most common method is the interaction between people and artwork, which is an emotional experience that static design work can also bring about; however, in the interaction between people and technology, dynamic graphics itself
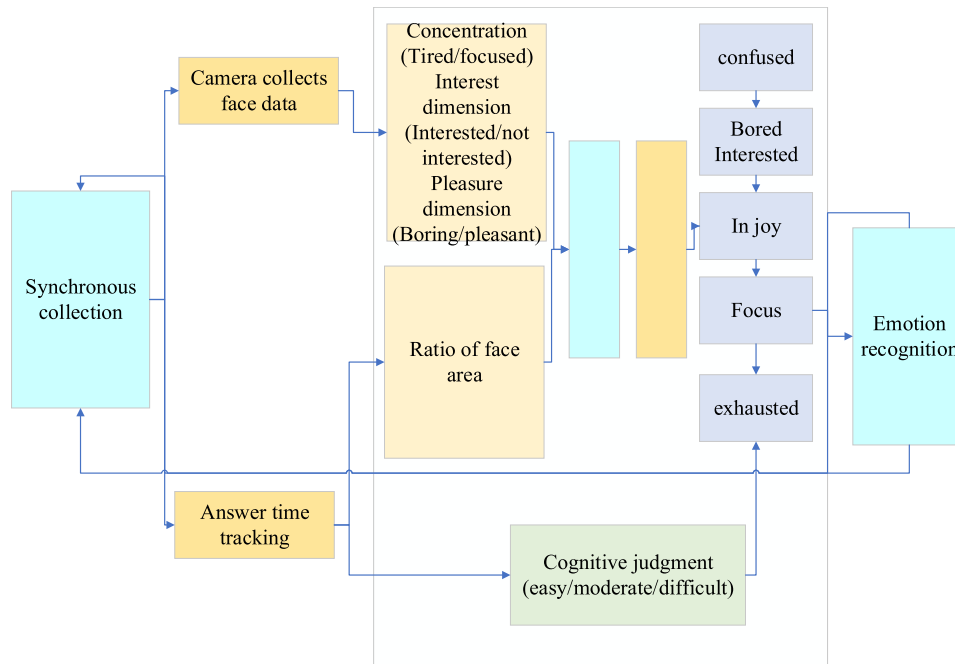
FIGURE 5. Evaluation of index design.

has a very good advantage in that it can make good use of a variety of media to develop, which is one of its unique properties.

The interaction between people and technology, of course, cannot be separated from the current hot technology, AR technology, which is a product of computer development and simulation of realistic scenes that results in a sense of immersion in the real environment experience. Through a combination of the virtual and realistic, the user can through some kind of device view the virtual environment by using AR glasses and mobile phones, for example. AR technology is used in a variety of fields and has certainly received attention from designers, who are bold enough to combine AR technology with still-face graphics, a new medium that has changed the form of posters from print media to a new medium.

Designers usually use AR to construct a more three-dimensional and realistic scenario where the still surface graphics look the same, but the AR device can be used to see the changing, dynamic graphics. The display of the work has an innovative form that is more interactive. By scanning the works through the mobile phone app, the original static works are added with kinetic and sound effects, creating a simulated situation and a different visual interactive experience, which is more interesting and brings different visual aesthetics that attract the audience in a more easy manner. When faced with new technology or brand-new visual content that has never been seen before, the audience will generally be brave enough to experience it to satisfy their curiosity, so they will receive good feedback. This kind of human-computer interaction experience brings powerful communication effects to design works and is also the trend of current design development, which has good development potential and consumer markets

in the future and brings more creative space to designers (Figure 5).

We should seek increasingly better design forms to integrate our emotions and information transfer into the output and seek all changes based on the same. We should try our best to make the situation as vivid, lively, and interesting as possible. Only works with emotional vitality can move the audience and leave a deep impression on them. In this chapter, we analyze the creation of contextual performance. There are various methods of contextual performance in motion graphics design, and the author attempts to divide them into three categories: contextual integration, virtual and real, and contextual interaction.

The memory in the image compression system includes program memory and data memory. The program memory stores the configuration file of the image compression FPGA, which determines the function of the FPGA and is not updated during orbit operation. Thus, the anti-fuse PROM, which is immune to single-particle effects, is used to store the power-up configuration file. The image compression system is based on the prediction-based LOCO-3D algorithm, which relies on the temporal and spatial correlation of pixels to remove redundancy and is very sensitive to errors, and even a single bit flip of the bitstream can lead to anomalous ground decoding. Therefore, the EDAC technique is adopted to verify the image cache SDRAM, and the RS error checking technique is used to verify the bitstream and increase the anti-single-particle capability of the memory.

For the image compression system, a ground test platform is designed to simulate the external interfaces such as camera transmission, ground decoding, power supply circuit, and telemetry remote control of the image compression system.
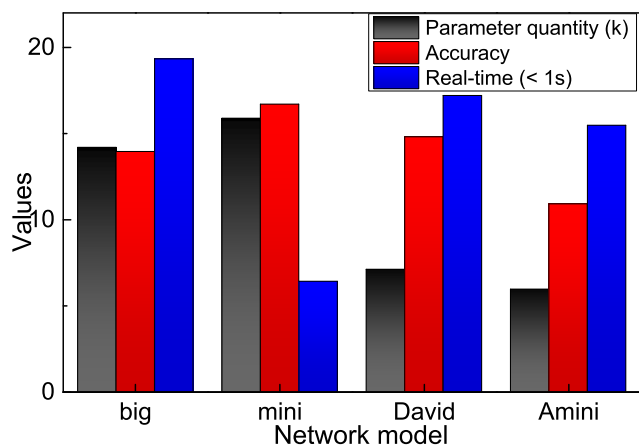
FIGURE 6. Performance comparison of different network models on dataset.

FIGURE 7. Comparison of performance of different structures.

The ground test platform is used for functional verification and performance evaluation of the image compression system. The encoder performance is comprehensively evaluated according to the encoder resources, power consumption, and pixel throughput rate. The real-time performance of the image compression system is verified according to the system compression delay. The anti-single-particle design of the system is verified through single-particle flip simulation experiments.

IV. RESULTS ANALYSIS

A. SYSTEM PERFORMANCE TEST RESULTS IN ANALYSIS

To evaluate the model recognition effect, this thesis mainly evaluates the training results by comparing several different algorithms on the homemade face dataset EA and the FER2013 dataset with a large amount of data collected from the Internet for real complex scenes. Figure 6 records the evaluation of the three improved models based on Xception and the overall network test results based on the Inception network model introduced in the literature.

As we can see in Figure 6, although the network model proposed by David Chan is more accurate for expression recognition in complex environments such as FER2013, the complex network structure and a large number of parameters do not guarantee the real-time requirements of the application, so all subsequent comparisons in this paper are based on the real-time requirements of the network model of a single case CNN. The results of the Fer2013 dataset show that the recognition efficiency of the A_mini_Xception network is not significantly improved. The reason may be related to the complexity of the data environment of the expression samples and the test results of the same network model, and the same parameters may also be affected by different experimental environments.

After the initial frame-trained model is obtained by the method in this chapter, subsequent training is mainly fine-tuned; i.e., the parameters of the initial model are kept constant, and the training updates the parameters of the feature transformation layer. To verify the role of the designed feature transformation layer, the experiments in this section compare
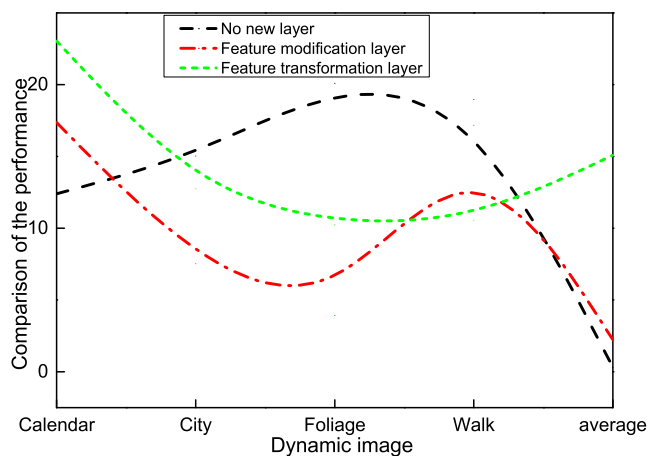
the three cases without the feature transformation layer, with the feature modification layer and with the feature transformation layer of this chapter, and quadruple magnification is used to calculate the average PSNR for Video4 to compare the performance differences. The results of the experiments are shown in Figure 7.

From Figure 7, it can be seen that the two methods of increasing the model depth of the network layers (the feature modification layer and the feature transformation layer) outperform the method of directly updating the underlying network parameters, while the improved feature transformation layer of this chapter achieves the best results in terms of objective metrics. Figure 7 shows a subjective rendering of the superresolution results of the three structured one-frame video images, and the superresolution results obtained using the feature transformation layer in this chapter are visually better than the other two methods. The feature transformation layer designed in this chapter is an effective network structure for improving the fine-tuning training effect.

This section also divides the test set into ideal double-triple downsampling and real-condition degradation downsampling. Since the same video is captured by the same transmission device, the degradation model of each frame is usually the same, so this section does not use different random fuzzy kernels and random noise degradation for each frame of the video in the test set as in Section 3.2. For comparison, this section uses 10 randomly generated fuzzy kernels to degenerate the videos in Video4 to simulate the different fuzzy down sampling processes, and 4 noise scenarios are constructed for the above low-resolution videos to account for the slight noise under real conditions.

A total of 180 videos with 180 sets of data overresolution results are averaged. The experimental results under ideal conditions are shown in Figure 8. It can be seen from Figure 8 that under ideal conditions, the method in this chapter exceeds the learning-based video superresolution method VSRnet in objective metrics and comes close to the VESPCN video superresolution method. The SOFVSR method achieves the best objective evaluation metrics due to
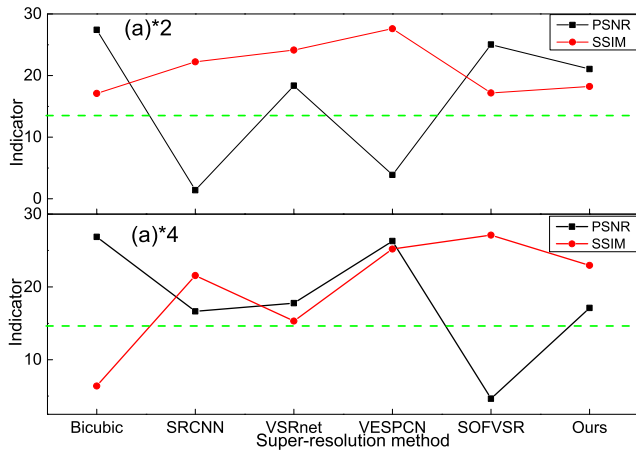
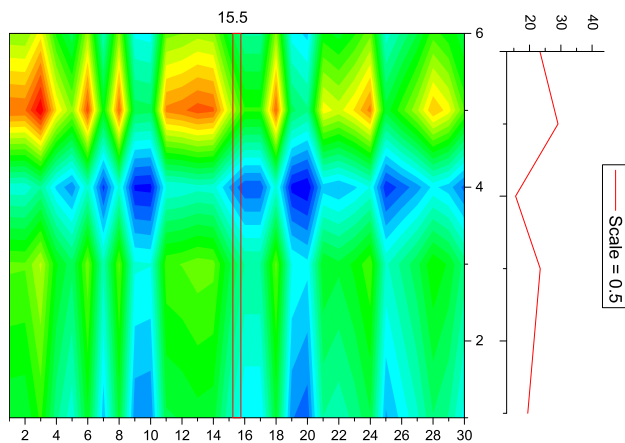**FIGURE 8.** Indicators of each algorithm under ideal conditions.

FIGURE 9. Comparison of superresolution results under ideal conditions for each frame of test set video.

FIGURE 10. Comparison of superresolution results for each frame of test set video under real conditions.

its good method design and the help of external training sets, but its neural network and the depth and complexity of the algorithms are high.

This section provides a detailed comparison of the PANS of each method for each video in the video test set for each frame of the image at fourfold magnification and plots the curves, as shown in Figure 9. From the curves, under ideal conditions, the SOFAS method's metrics for superresolution results lead on each frame of the video. The metrics of the method in this chapter are lower than those of VESNA in the beginning part of the video frames, but with incremental training, the model performance improves. For the image frames in the latter part of the video, the PAN of the method in this chapter is close to that of the VESNA method based on learning from a large number of external samples.

The metrics of each method under real degradation conditions are shown in Figure 10. The method presented in this chapter achieves the best objective metrics in a degenerate scenario with sampling under random fuzzy kernels and slight noise, while other superresolution methods used for comparison suffer a significant drop in performance due to noise and fuzzy interference. This section also plots a comparison curve of the average PSNR for each frame of the Video4 dataset
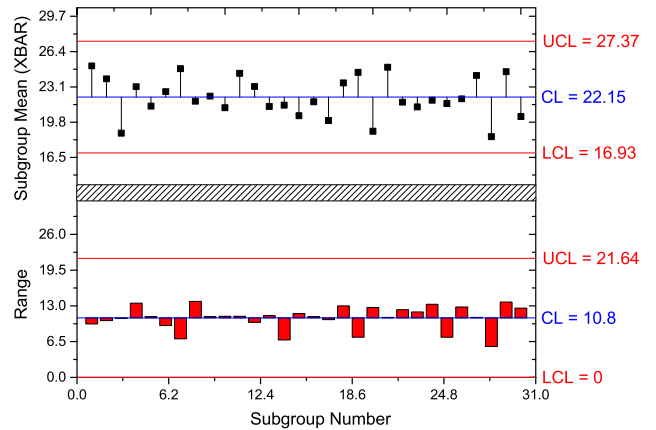
in a real degradation scenario, as shown in Figure 10. The PSNR curve clearly shows that the performance of the video superresolution method based on an external training dataset drops drastically in the face of nonideal video conditions, while the method in this chapter achieves better results in this scenario.

Figure 10 shows subjective comparison of the overresolution results of each method for video images in degraded scenes. The overresolution results of the method in this chapter overcome the blur to some extent, and the subjective effect is better than the other comparison methods. When slight noise is included, the video superresolution method based on external learning tends to amplify the noise more than the method in this chapter, making the image less subjective. The method in this chapter still achieves better visual results when facing video image frames with slight noise.

B. RESULTS ANALYSIS OF IMAGE FRAME FIXATION EVALUATION INDEX METHOD

When the user reaches any boundary of the tracking region during the tracking region walk, the system performs a reset operation, and we use S2C's freeze rotation method to handle collisions. For the algorithm in this paper, since we use a one-step-ahead strategy and a buffer to handle collisions, the user will be guided to steer along the buffer arc when entering the buffer. In rare cases, our algorithm will use the freeze steering method to handle conflicts.

We compare the number of times the two algorithms use freeze rotation and the path travel length in Figure 11. First, this algorithm can significantly reduce the number of reset operations, especially when the virtual space is much larger than the real space or in long walking paths. There are approximately 1100 collisions, but no collisions are generated by this algorithm. Second, since both methods ignore the short paths during the reset selection and the method also takes a growth path during the arc-in phase, the true path lengths of both methods are inaccurate, but the small weighting error is negligible for the total virtual path length. The true walk length of the method is 780 m. The true walk length of the method in this paper is 785.2 m.
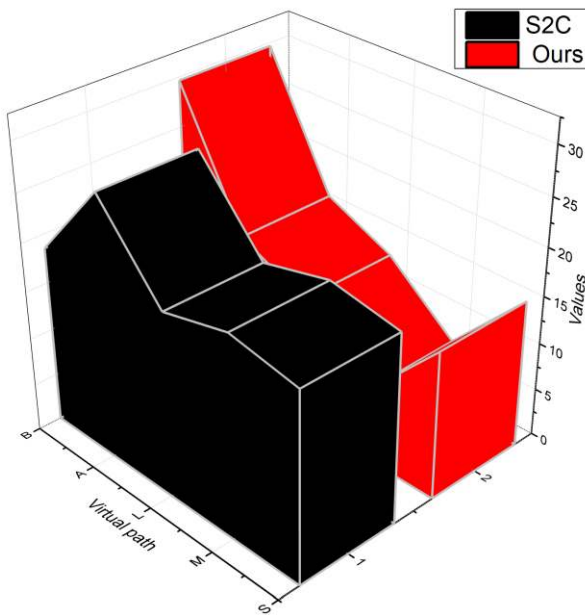
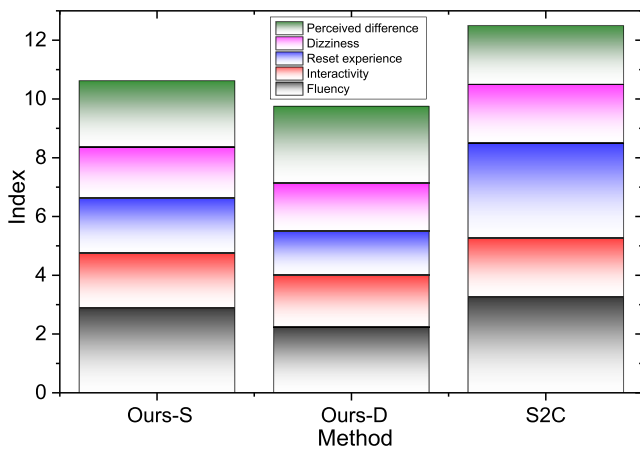**FIGURE 11.** Comparison of number of collisions.

FIGURE 12. Experiential evaluation.

The virtual path lengths are shown according to the small, medium, and large virtual spaces in Figure 12. Assuming the tracking area is 2.5 m × 2.5 m (A space), the roaming times using S2C are 53.45 s, 214.5 s, and 1556 s, while the times using this algorithm are 29.77 s, 166.5 s, and 899.7 s, respectively. Similarly, when the tracking area is 4 m × 4 m (B space), the roaming times using S2C were 53.45 s, 204.75 s, and 1456 s, respectively, compared to 27.7 s, 166.8 s, and 889.6 s using the algorithms in this paper. It is important to use real users to evaluate the performance of each algorithm.

Subject to the size of the physical space and the tracking capabilities of a single Kinect, we conducted comparison experiments only on the A-space and M-type virtual mazes. During VR navigation, the user wears a VR device consisting of cardboard and a smartphone to perceive the virtual space, which is rendered by the unity3D engine. The gyroscope sensor on the phone provides user orientation for our system,

and the Kinect and smartphone are connected to a PC, which is used to process the position and rotation data.

We kept the statistics of the three metrics mentioned earlier the same way that they were reset in the simulated experiments and obtained user experiment results similar to those in the simulations. Some users complained that both this paper and the S2C method produce large camera deflections, i.e., too much curvature gain, but it was more acceptable to walk large curvature arcs than to freeze the reset operation. Additionally, this method allows us to increase the buffer as the tracking area increases, thus reducing the curvature gain in the buffer area, which will help increase the user experience.

At the beginning of a virtual roam, we explain to the user what five metrics mean for better evaluation. The higher the score is, the better the experience is; and the lower the score is, the worse the experience is. The lower the score, the more vertigo-prone it is; the perceptual difference refers to the excessive deflection caused by excessive curvature gain. The higher the score, the stronger the sense of difference. From Figure 12, it can be seen that the dynamically rotated method of this paper can be rated higher; i.e., the reset operation has an important impact on the virtual roaming experience, and the dynamic steering algorithm of this paper effectively attenuates the visual interruption experience caused by freezing the scene.

Our S method reduces the number of collisions and improves the smoothness compared to the S2C method. Additionally, the term reset experience validates our findings, and users have a better assessment of the dynamic steering approach in this paper. For interactivity, there is a clear path from start to finish in our approach, and users point out that clear navigation leads to a better experience. For the vertigo-prone assessment, our method reduces the number of reset rotations and thus reduces vertigo, but the user's vertigo is not greatly improved due to the presence of larger curvature arcs. In this paper, we reduce the number of resets to reduce visual interruptions when the user performs virtual roaming, which improves the perceptual difference.

Using the feature fusion method described above at the introduction fusion time, the accuracy of each type of target object in the final dataset when the frame length k=9 before and after fusion is shown in Figure 13.

The accuracy of the method for fusing features is a slight improvement over the original optical flow algorithm. The original optical flow algorithm has an m AP≈0.748, while the method of fusing temporal features has an m AP≈0.778, which is roughly a four-percentage-point improvement. For specific object classes, the accuracy of the previous algorithm is relatively low for detecting classes such as monkeys, cars, and sheep. This is due to the blurred background and motion blocking phenomenon of these classes. In addition, its accuracy has been improved quite slightly.

When feature fusion is performed, different feature extraction networks and different frame lengths (k-values) before and after fusion result in different accuracy rates. The resent
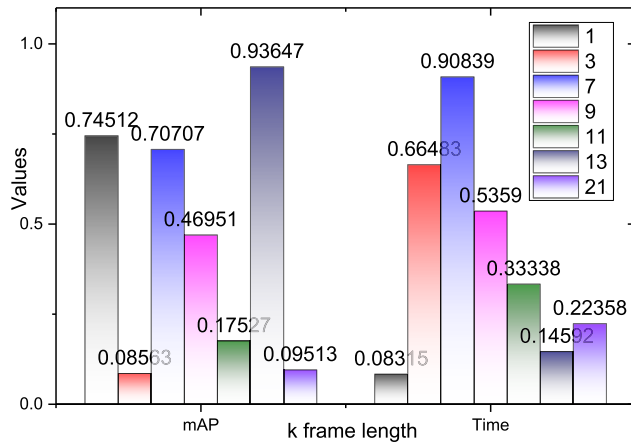
FIGURE 13. Detection results of feature fusion.

and resent time consumption relationships for different k-values are shown in Figure 13, while the accuracy rate relationship is shown in Figure 13, where the horizontal coordinate represents the keyframe scheduling interval. From Figure 13, for the same fusion feature-length k-values, the time consumption is less when using the resent network instead of the resent network, while the accuracy of resent is higher than that of resent. This is because resent has fewer network layers and less computation, which gives it an advantage in detection speed but the same accuracy as resent. The feature extraction capability is also weaker than that of resent, so it is at a disadvantage in terms of accuracy. This provides different options for realistic application requirements. For scenarios pursuing high accuracy, the resent network can be used to extract features, while for scenarios pursuing detection speed, the resent network is preferred for feature extraction.

V. CONCLUSION

An in-depth study of dynamic visual communication image framing for graphic design under a virtual reality environment was conducted. Application of the image compression system faced two challenges: "high-fidelity compression under limited bandwidth constraint" and "strong real-time compression under limited resource constraint." Based on the application scenarios of the image compression system, an integrated high-fidelity intraframe-to-frame-to-near lossless high-fidelity compression method was proposed. Based on the image high-fidelity compression method, an efficient parallel computing architecture based on FPGA was proposed. A system anti-single-particle design was proposed for the complex environment of a star, and a highly reliable and strong real-time image compression system was developed onboard the star.

For real-time implementation, an efficient hardware computing architecture for interframe lossless and near-lossless image compression was proposed in this paper. To solve the problem of large computational delays caused by context conflicts in the compression algorithm and pixel reconstruction loops in the near-lossless computation, the critical paths were optimized using multiple parallel computing structures

to reduce the computational delay. On this basis, the model construction method for geometric features was investigated in this paper. Using the kernel density estimation and conditional probability density estimation functions, the model fitted the probability distributions of different geometric features and then estimated the optimal element positions and colors under specific conditions.

Using the estimated geometric features, this paper further investigated the methods for generating flat images, including the multiline text layout generation method and the primary color-guided color reconstruction method. Additionally, to generate diverse design results, this paper investigated the clustering method of layouts and the visualization method of color-matching perceptual features and developed a corresponding flat image generation system to support designers in interactively optimizing design results. By comparing the design results of different methods and different objects, the experiments proved that the above models and methods can effectively realize graphic advertising image design and meet the aesthetic, functional, and personalized design needs of the target users.

REFERENCES

[1] H. Samih, "Smart cities and Internet of Things," *J. Inf. Technol. Case Appl. Res.*, vol. 21, no. 1, pp. 3–12, Jan. 2019.

[2] D.-H. Shin, "The role of affordance in the experience of virtual reality learning: Technological and affective affordances in virtual reality," *Telematics Informat.*, vol. 34, no. 8, pp. 1826–1836, Dec. 2017.

[3] Y. S. Yoon, H. Zo, M. Choi, D. Lee, and H.-W. Lee, "Exploring the dynamic knowledge structure of studies on the Internet of Things: Keyword analysis," *ETRI J.*, vol. 40, no. 6, pp. 745–758, Dec. 2018.

[4] C. E. Mora, J. Martín-Gutiérrez, B. Añorbe-Díaz, and A. González-Marrero, "Virtual technologies trends in education," *EURASIA J. Math., Sci. Technol. Edu.*, vol. 13, no. 2, pp. 469–486, Jan. 2017.

[5] N. Chung, H. Lee, J.-Y. Kim, and C. Koo, "The role of augmented reality for experience-influenced environments: The case of cultural heritage tourism in korea," *J. Travel Res.*, vol. 57, no. 5, pp. 627–643, May 2018.

[6] A. Milosavljević, D. Rančić, A. Dimitrijević, B. Predić, and V. Mihajlović, "Integration of GIS and video surveillance," *Int. J. Geograph. Inf. Sci.*, vol. 30, no. 10, pp. 2089–2107, Oct. 2016.

[7] S. C. H. Li, P. Robinson, and A. Oriade, "Destination marketing: The use of technology since the millennium," *J. Destination Marketing Manage.*, vol. 6, no. 2, pp. 95–102, Jun. 2017.

[8] N. Elmqaddem, "Augmented reality and virtual reality in education. Myth or reality?" *Int. J. Emerg. Technol. Learn.*, vol. 14, no. 3, pp. 234–242, Feb. 2019.

[9] G. Papanastasiou, A. Drigas, C. Skianis, M. Lytras, and E. Papanastasiou, "Virtual and augmented reality effects on K-12, higher and tertiary education students' twenty-first century skills," *Virtual Reality*, vol. 23, no. 4, pp. 425–436, Dec. 2019.

[10] M. Brengman, K. Willems, and H. Van Kerrebroeck, "Can't touch this: The impact of augmented reality versus touch and non-touch interfaces on perceived ownership," *Virtual Reality*, vol. 23, no. 3, pp. 269–280, Sep. 2019.

[11] M. Farshid, J. Paschen, T. Eriksson, and J. Kietzmann, "Go boldly!: Explore augmented reality (AR), virtual reality (VR), and mixed reality (MR) for business," *Bus. Horizons*, vol. 61, no. 5, pp. 657–663, Sep. 2018.

[12] D. tom Dieck, M. C. tom Dieck, T. Jung, and N. Moorhouse, "Tourists' virtual reality adoption: An exploratory study from lake district national park," *Leisure Stud.*, vol. 37, no. 4, pp. 371–383, Jul. 2018.

[13] S. Kang and S. Kang, "The study on the application of virtual reality in adapted physical education," *Cluster Comput.*, vol. 22, no. S1, pp. 2351–2355, Jan. 2019.

[14] F. Izzo, "Museum customer experience and virtual reality: H.BOSCH exhibition case study," *Modern Economy*, vol. 08, no. 04, pp. 531–536, 2017.

[15] N. M. D'Cunha, D. Nguyen, N. Naumovski, A. J. McKune, J. Kellett, E. N. Georgousopoulou, J. Frost, and S. Isbel, "A mini-review of virtual reality-based interventions to promote well-being for people living with dementia and mild cognitive impairment," *Gerontology*, vol. 65, no. 4, pp. 430–440, 2019.

[16] L. Qin, N. Yu, and D. Zhao, "Applying the convolutional neural network deep learning technology to behavioural recognition in intelligent video," *Tehnicki Vjesnik*, vol. 25, no. 2, pp. 528–535, 2018.

[17] X. Chen and J. Hu, "A review of haptic simulator for oral and maxillofacial surgery based on virtual reality," *Expert Rev. Med. Devices*, vol. 15, no. 6, pp. 435–444, Jun. 2018.

[18] J. H. Park, C. Lee, C. Yoo, and Y. Nam, "An analysis of the utilization of Facebook by local korean governments for tourism development and the network of smart tourism ecosystem," *Int. J. Inf. Manage.*, vol. 36, no. 6, pp. 1320–1327, Dec. 2016.

[19] P. Buonincontri and R. Micera, "The experience co-creation in smart tourism destinations: A multiple case analysis of European destinations," *Inf. Technol. Tourism*, vol. 16, no. 3, pp. 285–315, Sep. 2016.

[20] A. Darwish, A. E. Hassanien, M. Elhoseny, A. K. Sangaiah, and K. Muhammad, "The impact of the hybrid platform of Internet of Things and cloud computing on healthcare systems: Opportunities, challenges, and open problems," *J. Ambient Intell. Humanized Comput.*, vol. 10, no. 10, pp. 4151–4166, Oct. 2019.

[21] L. H. Son, S. Jha, R. Kumar, J. M. Chatterjee, and M. Khari, "Collaborative handshaking approaches between Internet of computing and Internet of Things towards a smart world: A review from 2009–2017," *Telecommun. Syst.*, vol. 70, no. 4, pp. 617–634, Apr. 2019.

[22] A. T. Chatfield and C. G. Reddick, "A framework for Internet of Things-enabled smart government: A case of IoT cybersecurity policies and use cases in U.S. Federal government," *Government Inf. Quart.*, vol. 36, no. 2, pp. 346–357, Apr. 2019.

[23] G. Misra, V. Kumar, A. Agarwal, and K. Agarwal, "Internet of Things (IoT)-a technological analysis and survey on vision, concepts, challenges, innovation directions, technologies, and applications (an upcoming or future generation computer communication system technology)," *Amer. J. Electr. Electron. Eng.*, vol. 4, no. 1, pp. 23–32, Feb. 2016.

[24] B. Li and Y. Li, "Internet of Things drives supply chain innovation: A research framework," *Int. J. Organizational Innov.*, vol. 9, no. 3, pp. 71–92, Jan. 2017.

[25] C. K. Ng, C. H. Wu, K. L. Yung, W. H. Ip, and T. Cheung, "A semantic similarity analysis of Internet of Things," *Enterprise Inf. Syst.*, vol. 12, no. 7, pp. 820–855, Aug. 2018.

[26] C. T. Lai, P. R. Jackson, and W. Jiang, "Shifting paradigm to service-dominant logic via Internet-of-Things with applications in the elevators industry," *J. Manage. Anal.*, vol. 4, no. 1, pp. 35–54, Jan. 2017.

[27] Y.-C. Chen, "A tutorial on kernel density estimation and recent advances," *Biostatistics Epidemiology*, vol. 1, no. 1, pp. 161–187, Jan. 2017.

[28] H. Lee, O. Na, Y. Kim, and H. Chang, "A study on designing public safety service for Internet of Things environment," *Wireless Pers. Commun.*, vol. 93, no. 2, pp. 447–459, Mar. 2017.

[29] W. Serrano, "Digital systems in smart city and infrastructure: Digital as a service," *Smart Cities*, vol. 1, no. 1, pp. 134–154, Dec. 2018.

[30] S. N. V. Yuan and H. H. S. Ip, "Using virtual reality to train emotional and social skills in children with autism spectrum disorder," *London J. Primary Care*, vol. 10, no. 4, pp. 110–112, Jul. 2018.

[31] H. Habibzadeh, K. Dinesh, O. Rajabi Shishvan, A. Boggio-Dandry, G. Sharma, and T. Soyata, "A survey of healthcare Internet of Things (HIoT): A clinical perspective," *IEEE Internet Things J.*, vol. 7, no. 1, pp. 53–71, Jan. 2020.

[32] S. Balakrishnan, S. S. Rani, and K. C. Ramya, "Design and development of IoT based smart aquaculture system in a cloud environment," *Int. J. Oceans Oceanogr.*, vol. 13, no. 1, pp. 121–127, Oct. 2019.

[33] P. M. Kumar, U. Gandhi, R. Varatharajan, G. Manogaran, R. Jidhesh, and T. Vadivel, "Intelligent face recognition and navigation system using neural learning for smart security in Internet of Things," *Cluster Comput.*, vol. 22, no. S4, pp. 7733–7744, Jul. 2019.

[34] A. A. A. Sen, F. A. Eassa, K. Jambi, and M. Yamin, "Preserving privacy in Internet of Things: A survey," *Int. J. Inf. Technol.*, vol. 10, no. 2, pp. 189–200, Jun. 2018.

[35] C. Gomez, S. Chessa, A. Fleury, G. Roussos, and D. Preuveneers, "Internet of Things for enabling smart environments: A technology-centric perspective," *J. Ambient Intell. Smart Environments*, vol. 11, no. 1, pp. 23–43, Jan. 2019.

ZHIYONG TIAN was born in Zhengzhou, China, in 1981. He graduated from the Hubei University of Technology, where he received the master's degree in architecture and environment. He is currently an Associate Professor and the Vice Dean with the Art College, Henan University of Animal Husbandry and Economics. He is also one of the young and middle-aged backbone teachers in Henan. He has hosted and participated in three projects at provincial and ministerial level, five projects at prefectural and departmental level, and two projects at school level. He has published more than 15 academic articles (works), completed one monograph, participated in compiling two textbooks, presided over the completion of two national invention patents, and one national utility model patent. He is a member of the Communist Party of China. He is also a member of the Education Committee, the 15th (Zhengzhou) Professional Committee of Interior Design Branch of Architectural Society of China, a member of the Henan Packaging Technology Association, and a Judge of the Oriental Creative Star Design Competition.

• • •